

## ARTICLE

# CO hydrogenation over K-Co-MoS<sub>x</sub> catalyst to mixed alcohols: A kinetic analysis

Leila Negahdar<sup>1,3</sup> | Xiaoying Xi<sup>2</sup> | Feng Zeng<sup>1</sup> | J. G. M. Winkelman<sup>2</sup> | Hero Jan Heeres<sup>2</sup> | Regina Palkovits<sup>1</sup>

<sup>1</sup> Heterogeneous Catalysis and Technical Chemistry, RWTH Aachen University, Aachen 52074, Germany

<sup>2</sup> Green Chemical Reaction Engineering, Engineering and Technology Institute Groningen, University of Groningen, Nijenborgh 4, Groningen 9747AG, The Netherlands

<sup>3</sup> Department of Chemistry, UCL, London WC1H 0AJ, UK

## Correspondence

Hero Jan Heeres, Green Chemical Reaction Engineering, Engineering and Technology Institute Groningen, University of Groningen, Nijenborgh 4, Groningen, AG 9747, The Netherlands.

Email: [h.j.heeres@rug.nl](mailto:h.j.heeres@rug.nl)

Regina Palkovits, Chair of Heterogeneous Catalysis and Technical Chemistry, RWTH Aachen University, Worringerweg 2, Aachen 52074, Germany.

Email: [palkovits@itmc.rwth-aachen.de](mailto:palkovits@itmc.rwth-aachen.de)

## Funding information

China Scholarship Council; Excellence Initiative of the German Federal and State Governments

## Abstract

Higher alcohol synthesis (HAS) from syngas is one of the most promising approaches to produce fuels and chemicals. Our recent investigation on HAS showed that potassium-promoted cobalt-molybdenum sulfide is an effective catalyst system. In this study, the intrinsic kinetics of the reaction were studied using this catalyst system under realistic conditions. The study revealed the major oxygenated products are linear alcohols up to butanol and methane is the main hydrocarbon. The higher alcohol products (C<sub>3</sub>+) followed an Anderson-Schultz-Flory distribution while the catalyst suppressed methanol and ethanol formation. The optimum reaction conditions were estimated to be at temperature of 340°C, pressure of 117 bar, gas hourly space velocity of 27 000 mL g<sup>-1</sup> h<sup>-1</sup> and H<sub>2</sub>/CO molar feed ratio of 1. A kinetic network has been considered and kinetic parameters were estimated by nonlinear regression of the experimental data. The results indicated an increasing apparent activation energy of alcohols with the length of alcohols except for ethanol. The lower apparent activation energy of alcohols compared with hydrocarbon evidenced the efficiency of this catalyst system to facilitate the formation of higher alcohols.

## KEYWORDS

carbon chain growth, kinetics, mechanism, mixed alcohols, molybdenum disulfide, syngas

**Abbreviations:**  $F_i$ , molar flow of component  $i$  (mol s<sup>-1</sup>);  $K_{WGS}$ , equilibrium constant;  $y_i$ , molar composition of component  $i$ ;  $y_n$ , mole fraction of alcohol;  $A_i$ , pre-exponential factor (kmol/(kg s bar<sup>Σ<sub>reaction orders</sub></sup>));  $C_{Mears}$ , Mears criterion;  $C_{WP}$ , Weisz-Prater criterion;  $E_a$ , activation energy (kJ mol<sup>-1</sup>); GHSV, Gas hourly space velocity (mL g<sup>-1</sup> h<sup>-1</sup>); HAS, higher alcohols synthesis;  $k$ , reaction rate constant (s<sup>-1</sup>);  $n$ , carbon number;  $P$ , pressure (bar);  $r$ , reaction rate (mol m<sup>-3</sup> s<sup>-1</sup>);  $T$ , temperature (K);  $W$ , mass of catalyst (kg);  $\alpha$ , chain-growth probability

This is an open access article under the terms of the [Creative Commons Attribution-NonCommercial-NoDerivs](https://creativecommons.org/licenses/by-nc-nd/4.0/) License, which permits use and distribution in any medium, provided the original work is properly cited, the use is non-commercial and no modifications or adaptations are made.

© 2020 Wiley Periodicals LLC

## 1 | INTRODUCTION

The thermochemical conversion of biomass to synthesis gas, followed by catalytic conversion of synthesis gas to higher alcohols (HAs), offers an attractive and promising source of renewable energy.<sup>1,2</sup> HAs contain two or more carbon atoms including primary and secondary alcohols of both linear and branched carbon chains. HAs from C<sub>2</sub> to C<sub>5</sub> can be used directly as transportation fuels, as octane and cetane enhancers and

environmentally friendly fuel additives, as specialty solvents in, for example, cleaning agents and paint industry, and as intermediates for manufacture of pharmaceuticals and plastics.<sup>3–6</sup>

A wide variety of heterogeneous catalysts have been developed for the conversion of syngas into HA.<sup>2</sup> Among the various catalysts, Mo-based catalysts are considered the most promising due to their high activity and selectivity for alcohol formation and being excellent catalysts for the water–gas shift reaction. Particularly, MoS<sub>2</sub>-based catalysts developed by Dow Chemical possess several advantages such as high resistance to sulfur poisoning and high selectivity to linear alcohols.<sup>7–10</sup> However, the addition of alkali metals is required to suppress or minimize the hydrogenation activity of surface alkyl species forming alkanes and to enhance the performance of catalysts toward HAs.<sup>7,11</sup> Previous studies emphasized that addition of transition metals such as Co, Ni, and Fe to the alkali-promoted MoS<sub>2</sub> enhances the selectivity of HA,<sup>9,12,13</sup> among which Co is the most effective promoter for higher yield of HAs.<sup>14</sup> The major oxygenated products over these catalysts include linear alcohols also carbon distributions usually follow the Anderson-Schultz-Flory (ASF) distribution.<sup>14,15</sup>

Our recent investigation also showed that cobalt-molybdenum sulfide promoted by potassium is an effective catalyst system for HA synthesis.<sup>16</sup> Detailed study on the role of potassium and cobalt in K-modified CoMoS<sub>x</sub> catalysts and their promotional effects on the selectivity of HAs have been reported by our group.<sup>17</sup> In this study, we aimed to analyze the kinetics of mixed alcohol synthesis over this catalyst system enabling an insight into the reaction and providing information applicable for reactor design and process optimization. The effects of operating conditions such as temperature, pressure, gas hourly space velocity, and H<sub>2</sub>/CO molar feed ratio on HA selectivity have been investigated. Further, the reaction kinetic parameters were estimated to explain the catalytic activity of CO hydrogenation over potassium promoted cobalt molybdenum disulfide.

## 2 | EXPERIMENTAL

### 2.1 | Catalyst preparation

The cobalt-molybdenum oxide precursor was prepared by dissolving 2.83 g Co(NO<sub>3</sub>)<sub>2</sub>·6H<sub>2</sub>O and 17.170 g (NH<sub>4</sub>)<sub>6</sub>Mo<sub>7</sub>O<sub>24</sub>·4H<sub>2</sub>O in 50 mL deionized water, followed by heating at 120°C to evaporate the water. After that, the obtained mixture was calcined in air at 500°C for 3 h to form cobalt-molybdenum oxide. The cobalt-molybdenum

sulfide was prepared by the sulfurization of cobalt-molybdenum oxide with potassium thiocyanate (KSCN). Typically, 0.648 g cobalt-molybdenum oxide, 0.875 g KSCN, and 35 mL deionized water were mixed in an autoclave. The autoclave was kept at 200°C for 24 h. The autoclave was cooled, and the precipitate was filtered and washed with deionized water to remove the impurities. After drying at ambient conditions overnight, cobalt-molybdenum sulfide (Co<sub>0.13</sub>Mo<sub>0.87</sub>S<sub>1.76</sub>) was determined by inductively coupled plasma - optical emission spectrometry (ICP-OES) analysis. The detailed characterization data of this catalyst can be found elsewhere.<sup>16</sup>

### 2.2 | Experimental procedure

The catalytic reactions were carried out in a high-pressure fixed bed reactor (10 mm inner diameter). The gas mixture with a H<sub>2</sub>/CO/N<sub>2</sub> volume ratio of 55:36.7:8.3 and H<sub>2</sub>/CO of 1.5 was mixed and pressurized by a high-pressure compressor before entering the reactor. The flow rate of gas mixture was controlled using a high-pressure mass flow controller. The reactor was placed in an oven to keep the reaction temperature constant. The exit stream from the reactor was cooled and separated by a double walled condenser at –5°C. Cobalt-molybdenum sulfide (0.394 g) and 0.056 g K<sub>2</sub>CO<sub>3</sub> were mixed and grinded in a mortar, and 0.4 g of the mixture was diluted with 3.0 g SiC before loading in the reactor. Before syngas reaction experiment, the catalyst mixture was pretreated in H<sub>2</sub> flow of 50 mL min<sup>–1</sup> at 450°C and for 8 h. The stability of the optimal catalyst was tested at 340°C, 117 bar, H<sub>2</sub>/CO = 1.5, and 4 500 mL g<sup>–1</sup> h<sup>–1</sup> and the result showed that stable CO conversion and product selectivity could be obtained after an induction period of 20 h. Therefore, samples were collected after 20 h and analyzed by average of 6 h runtime, to ensure that reactor was operated at steady-state conditions. The gas products were analyzed by an online gas chromatograph (Compact GC; Interscience BV, Breda, the Netherlands). The liquid products were analyzed by an offline gas chromatograph (Finnigan TRACE GC Ultra; Thermo Scientific, Eindhoven, the Netherlands). Details regarding product analysis are described in our previous publication.<sup>16</sup> The following ranges of operating conditions were explored: temperature 340–380°C; total pressure, 87–147 bar; gas hourly space velocity (GHSV) 4 500–27 000 mL g<sup>–1</sup> h<sup>–1</sup> and H<sub>2</sub>/CO molar feed ratio of 1–2. For all experiments, a carbon balance closure higher than 95% was obtained and the selectivity of all products is mole (carbon) based. Several duplicate experiments were performed (Table S1) confirming the reproducibility (±5% relative) of results. The CO conversion (X<sub>CO</sub>) and the

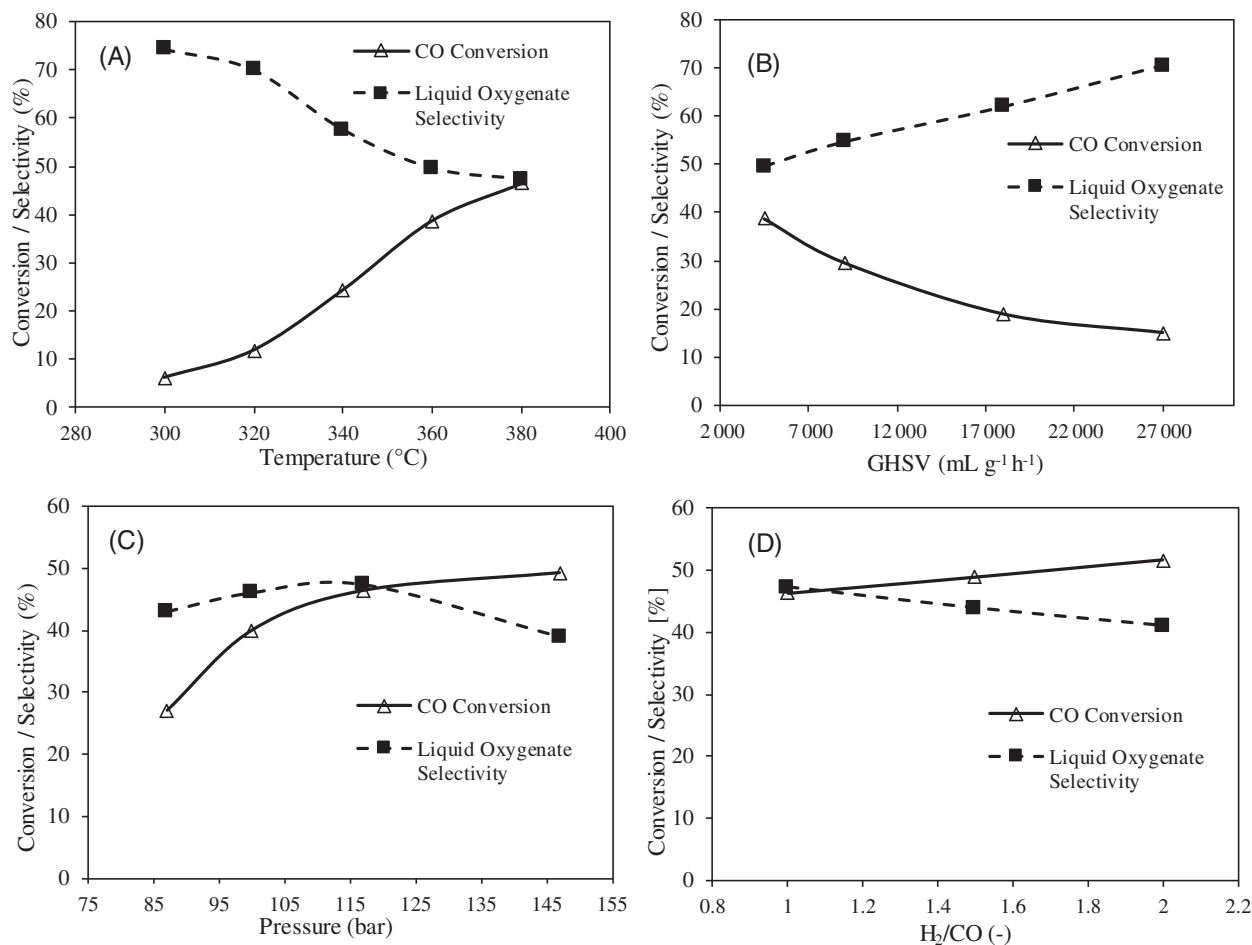


**FIGURE 1** Effects of reaction conditions on CO conversion and liquid oxygenate selectivity; reaction conditions: (A)  $P = 117$  bar,  $H_2/CO = 1$ ,  $GHSV = 4\,500\text{ mL g}^{-1}\text{ h}^{-1}$ ; (b)  $P = 117$  bar,  $T = 360^\circ\text{C}$ ,  $H_2/CO = 1$ ; (C)  $GHSV = 4\,500\text{ mL g}^{-1}\text{ h}^{-1}$ ,  $T = 380^\circ\text{C}$ ,  $H_2/CO = 1$ ; (D)  $GHSV = 4\,500\text{ mL g}^{-1}\text{ h}^{-1}$ ,  $T = 380^\circ\text{C}$ ,  $P = 117$  bar

product selectivity ( $S_i$ ) were calculated using Equations (1) and (2):

$$X_{CO} = \frac{\text{moles of CO}_{\text{influent}} - \text{moles of CO}_{\text{effluent}}}{\text{moles of CO}_{\text{influent}}} \times 100\% \quad (1)$$

$$S_i = \frac{\text{moles of product } i \times \text{number of carbons in product } i}{\text{moles of CO}_{\text{influent}} - \text{moles of CO}_{\text{exfluent}}} \times 100\% \quad (2)$$

### 3 | RESULTS AND DISCUSSION

#### 3.1 | Effects of reaction conditions on CO conversion and liquid oxygenate selectivity

The effects of reaction conditions on CO conversion and liquid oxygenate selectivity were investigated (Figure 1). The liquid oxygenates include alcohols (mainly C1-C4)

and very small amounts of acetaldehyde. The liquid oxygenate selectivity exhibits a maximum at reaction temperature of  $300^\circ\text{C}$  and decreases with increasing reaction temperature (Figure 1A). This indicates that CO hydrogenation becomes less selective toward liquid oxygenates with increasing reaction temperatures and it favors the formation of alkanes. However, the increase in GHSV has a positive effect on the selectivity of liquid oxygenates (Figure 1B). Higher GHSV means shorter contact time between reacting species and catalyst. With longer contact time, liquid oxygenates might be further converted to hydrocarbons. Therefore, the selectivity of liquid oxygenates increases with higher GHSV. The effect of pressure indicates that pressures below and at 117 bar are the most effective to maximize the liquid oxygenate selectivity and pressure above 117 bar favors hydrocarbon formation (Figure 1C).

The influence of the  $H_2/CO$  molar feed ratio on the selectivity of liquid oxygenates indicates that the selectivity decreases linearly with higher  $H_2/CO$  molar feed ratios

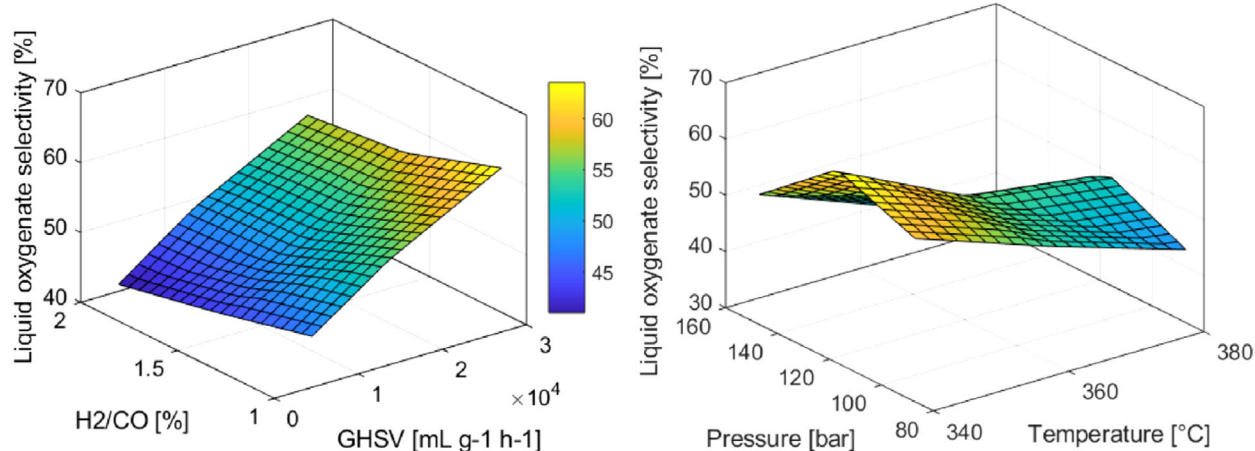


FIGURE 2 3D Plot of reaction conditions (liquid temperature, pressure, H<sub>2</sub>/CO ratio, and GHSV) [Color figure can be viewed at wileyonlinelibrary.com]

as shown in Figure 1D. At higher H<sub>2</sub>/CO molar ratio, the rate of chain growth by CO insertion decreases and higher hydrogen partial pressures supports the hydrogenation of intermediates to hydrocarbons.<sup>17</sup> As such, the selectivity of liquid oxygenates decreases at higher H<sub>2</sub>/CO molar ratio.

The increase in the reaction temperature, pressure, and H<sub>2</sub>/CO molar feed ratio has positive effects on CO conversion but higher GHSV does not favor the CO conversion due to short contact time between reactants and catalyst.

To investigate the optimum reaction conditions for higher selectivity of liquid oxygenate, the selectivity of liquid oxygenates with respect to the reaction conditions has been plotted in Figure 2. The 3D plot indicates that the optimum conditions become evident at reaction temperature around 340°C, pressure of 117 bar, GHSV above 27 000 mL g<sup>-1</sup> h<sup>-1</sup>, and H<sub>2</sub>/CO molar feed ratio of 1.

In this study, alcohol product distribution followed the so-called ASF distributions. Based on ASF distribution,<sup>18</sup> if the hydrocarbon chain is formed step-wise by insertion or addition of C<sub>1</sub> intermediates with constant growth probability then the chain length distribution can be defined as Equations (3) and (4)<sup>19</sup>:

$$y_n = (1 - \alpha) \alpha^{n-1} \quad (3)$$

$$\ln(y_n) = \ln\left(\frac{1}{\alpha} - 1\right) + n \ln(\alpha) \quad (4)$$

where  $y_n$  is the mole fraction of alcohol or hydrocarbon,  $n$  is the carbon number, and  $\alpha$  is the chain-growth probability. Figure 3 illustrates the ASF distributions of alcohols at the operating conditions of 340, 360, and 380°C, 117 bar, GHSV of 27 000 mL g<sup>-1</sup> h<sup>-1</sup>, and a H<sub>2</sub>/CO ratio of 1.5. Experimental observations show that the formation of alcohols except for methanol and ethanol, decreases exponentially with increasing carbon number, in agreement

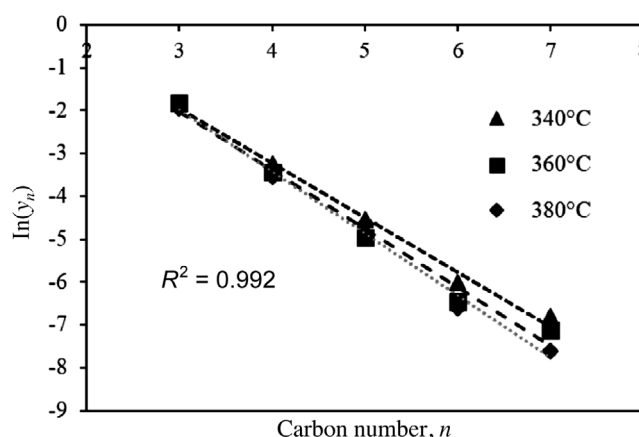


FIGURE 3 ASF distribution of alcohols for C<sub>3+</sub>, at 340, 360, and 380°C, 117 bar, GHSV of 27 000 mL g<sup>-1</sup> h<sup>-1</sup> and H<sub>2</sub>/CO = 1.5

with an ASF distribution. The chain growth probabilities for alcohols were estimated to be 0.13, 0.11, and 0.09 at temperatures of 340, 360, and 380°C, respectively, which were obtained based on C<sub>3+</sub> alcohols. The chain growth probabilities decrease with increasing reaction temperature, implying that HAS is unfavorable at higher temperature. This is in line with our experimental analysis of effects of reaction temperature on selectivity of liquid oxygenates.

### 3.2 | Internal and external diffusion effects

The Weisz-Prater criterion ( $C_{WP}$ ) was used to determine possible internal mass transfer limitations. In general, internal mass-transfer limitations can be neglected in case the  $C_{WP} \ll 1$ .<sup>20</sup> The value of  $C_{WP}$  was calculated to be 0.142, considering an average particle diameter of 105 μm and a

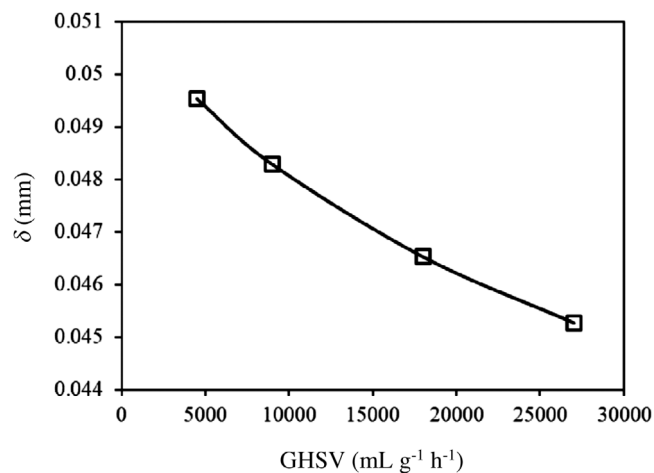


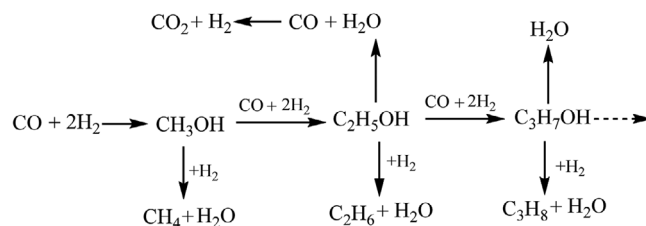
FIGURE 4 Effect of GHSV on boundary layer thickness around catalyst particle ( $\delta$ ) at 360°C, 117 bar,  $H_2/CO = 1$

$CO/H_2$  molar ratio of 1, indicating that internal diffusion is negligible (Supporting Information). External mass transfer limitations were verified experimentally by varying the GHSV at constant reaction conditions.<sup>21,22</sup> The external mass transfer diffusion can be eliminated by decreasing the mass-transfer boundary layer thickness (Supporting Information), which will disappear at high GHSV.<sup>22</sup> GHSV of 4 500, 9 000, 18 000, and 27 000  $mL\ g^{-1}\ h^{-1}$  were used at 360°C, 117 bar of syngas with a  $H_2/CO$  ratio of 1, and an averaged catalyst particle size of 105  $\mu m$  to test the presence of external mass transfer limitation. At low GHSV, the boundary layer across which the reactant diffuses is thick, and it takes a long time for reactants to diffuse to the surface of the catalyst. Therefore, mass transfer across the boundary layer is slow and limits the rate of the overall reaction. On the other hand, when the GHSV increases, the velocity over the pellet increases which results in a thinner boundary layer and the mass transfer rate increases. Accordingly, external mass transfer no longer limits the rate of reaction (Figure 4).<sup>21</sup>

An alternative criterion to determine the influence of external diffusion on the overall kinetics is the Mears criterion ( $C_{Mears}$ ).<sup>23</sup> External mass transport limitations are absent when the value of  $C_{Mears} \ll 0.15$ . The Mears criterion was calculated to be  $1.95 \times 10^{-5}$  (at equal molar ratio of CO and  $H_2$ ), which indicates that external mass transfer limitation can be excluded, which is in line with the experimental data obtained by variation of the GHSV (Supporting Information).

### 3.3 | Reaction network and kinetic model development

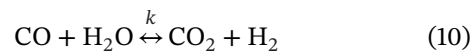
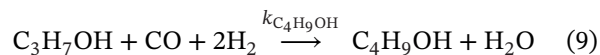
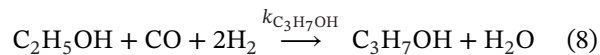
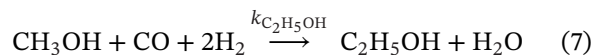
The mechanism of synthesis gas conversion over Mo-based catalysts has been the subject of debate in recent years. Var-



SCHEME 1 Parity plot of the experimental and model flow rates for the different components

ious kinetic models and mechanistic proposals have been made regarding HAS.<sup>19,24–28</sup> The widely accepted mechanism for alcohol formation over  $MoS_2$  catalysts is the CO insertion mechanism proposed by Santiesteban et al,<sup>14</sup> which was verified by isotopic labeling studies. The proposed mechanism comprehends the insertion of CO to the surface alkyl group ( $CH_3^*$ ) to form an acyl intermediate ( $CH_3CO^*$ ), which is then hydrogenated to the corresponding alcohol or to a longer alkyl group. Hydrocarbons are then formed by hydrogenation of the alkyl group. The overall reaction network for linear alcohols from syngas based on the CO insertion mechanism is shown in the Scheme 1.

Kinetic models for HAS over  $MoS_2$  catalysts are limited and some of them require complex formulations,<sup>19,27</sup> which might not be practical for the process design. Accordingly, in this study, the reaction schemes and rate expressions were simplified and CO insertion mechanism proposed by Santiesteban et al<sup>14</sup> is assumed. The reaction steps are summarized in Equations (5)–(10):



Higher alcohol ( $C_{2+}$ ) formation is assumed to proceed by a stepwise chain growth of alcohols by CO insertion into a lower molecular weight alcohol, whereas methanol is formed directly from syngas. The water-gas shift reaction (Equation 10) is known to be reversible and the other

reactions are assumed to be irreversible under high CO conversion. It is assumed that the hydrocarbons are formed by hydrogenation of the corresponding alcohols. Note that in the product mixture, mostly linear alcohols, small amount of branched propanol and butanol, methane, carbon dioxide, un-reacted carbon monoxide, and hydrogen were observed. It should be mentioned that the water concentration was about 10% of the overall liquid products, which is negligible. For kinetic model development, a power-law approach was applied.<sup>19,27,30–32</sup> Reaction rates of the individual compounds are expressed as follows:

$$r_{\text{CH}_3\text{OH}} = k_{\text{CH}_3\text{OH}} p_{\text{CO}}^a p_{\text{H}_2}^b \quad (11)$$

$$r_{\text{CH}_4} = k_{\text{CH}_4} p_{\text{CH}_3\text{OH}}^c p_{\text{H}_2}^d \quad (12)$$

$$r_{\text{C}_2\text{H}_5\text{OH}} = k_{\text{C}_2\text{H}_5\text{OH}} p_{\text{CH}_3\text{OH}}^e p_{\text{CO}}^f p_{\text{H}_2}^g \quad (13)$$

$$r_{\text{C}_3\text{H}_7\text{OH}} = k_{\text{C}_3\text{H}_7\text{OH}} p_{\text{C}_2\text{H}_5\text{OH}}^h p_{\text{CO}}^i p_{\text{H}_2}^j \quad (14)$$

$$r_{\text{C}_4\text{H}_9\text{OH}} = k_{\text{C}_4\text{H}_9\text{OH}} p_{\text{C}_3\text{H}_7\text{OH}}^k p_{\text{CO}}^l p_{\text{H}_2}^m \quad (15)$$

First-order reversible kinetics are assumed for the formation of CO<sub>2</sub> by the water-gas shift reaction (Equation 16)<sup>33,34</sup>:

$$r_{\text{CO}_2} = k p_{\text{CO}} - \left( \frac{k}{K_{\text{WGS}}} \right) p_{\text{CO}_2} \quad (16)$$

where  $k$  is reaction rate constant and  $K_{\text{WGS}}$  is the equilibrium constant that can be calculated from Equation (17)<sup>33</sup>:

$$K_{\text{WGS}} = \exp \left[ \left( \frac{4577.8}{T} \right) - 4.33 \right]. \quad (17)$$

### 3.4 | Reactor modeling

It is assumed that reactor follows the ideal plug-flow conditions and operates isothermally. With these assumptions, the mole balances for the individual components can be derived (Equations 18–26).

$$\frac{dF_{\text{CO}}}{dW} = - (r_{\text{Me}} + r_{\text{Et}} + r_{\text{Pr}} + r_{\text{CO}_2}) \quad (18)$$

$$\frac{dF_{\text{H}_2}}{dW} = - (2r_{\text{Me}} + 2r_{\text{Et}} + 2r_{\text{Pr}} + r_{\text{CH}_4}) + r_{\text{CO}_2} \quad (19)$$

$$\frac{dF_{\text{H}_2\text{O}}}{dW} = r_{\text{Et}} + r_{\text{Pr}} + r_{\text{CH}_4} - r_{\text{CO}_2} \quad (20)$$

$$\frac{dF_{\text{Me}}}{dW} = r_{\text{Me}} - r_{\text{Et}} - r_{\text{CH}_4} \quad (21)$$

$$\frac{dF_{\text{Et}}}{dW} = r_{\text{Et}} - r_{\text{Pr}} \quad (22)$$

$$\frac{dF_{\text{Pr}}}{dW} = r_{\text{Pr}} \quad (23)$$

$$\frac{dF_{\text{Bu}}}{dW} = -r_{\text{Pr}} \quad (24)$$

$$\frac{dF_{\text{CH}_4}}{dW} = r_{\text{CH}_4} \quad (25)$$

$$\frac{dF_{\text{CO}_2}}{dW} = r_{\text{CO}_2} \quad (26)$$

where  $W$  is the mass of catalyst and  $F_i$  is the molar flow of component  $i$ . The parameter estimation was performed by minimizing the objective function ( $Q$ ), which is defined as the sum of the squares of the residuals (Equation 27):

$$Q = \sum_{i=1}^N \sum_{j=1}^M (F_{ij(\text{model})} - F_{ij(\text{experiment})})^2 \quad (27)$$

where  $F_{ij}$  is the molar flow of compound  $i$  at the outlet of the reactor for experiment number  $j$ ,  $N$  is the number of experiments, and  $M$  the number of compounds. Our objective is to find the rate constants such that the molar flow obtained by integrating the differential equations (Equations 18–26) resembles the experimental molar flow as closely as possible. This is accomplished through an optimization procedure that we implemented in MATLAB using a general-purpose finite difference solver combined with MATLAB's native optimization routines. These routines are based on the method of least squares, employing a trust region reflective search algorithm. Figure 5 shows the fit between experimental and the predicted model values. The  $R^2$  values of the models emphasize a good fit with the experimental results. Table 1 summarizes the estimated kinetic parameters for the different reactions. The results indicate the activation energy increases with the length of alcohols except for ethanol. The lower value of apparent activation energy of ethanol compared with those for other alcohols was also reported by Gunturu et al.,<sup>19</sup> which was attributed to the ethanol conversion to products such as esters and ethers at higher reaction temperature. Methane and carbon dioxide have higher activation energy than alcohols. This also explains that the potassium promoted cobalt-molybdenum sulfide catalyst system favors the HAS formation compared with hydrocarbons as a result of lower activation energies of alcohols. In other words, this catalyst system facilitates the formation of HAS. Overall, a good agreement between the estimated kinetic parameters in this study and the reported range of data in the literature can be seen. Nevertheless, the estimated kinetic parameters can provide information required for simulation of commercial reactor, which will be addressed in future studies.

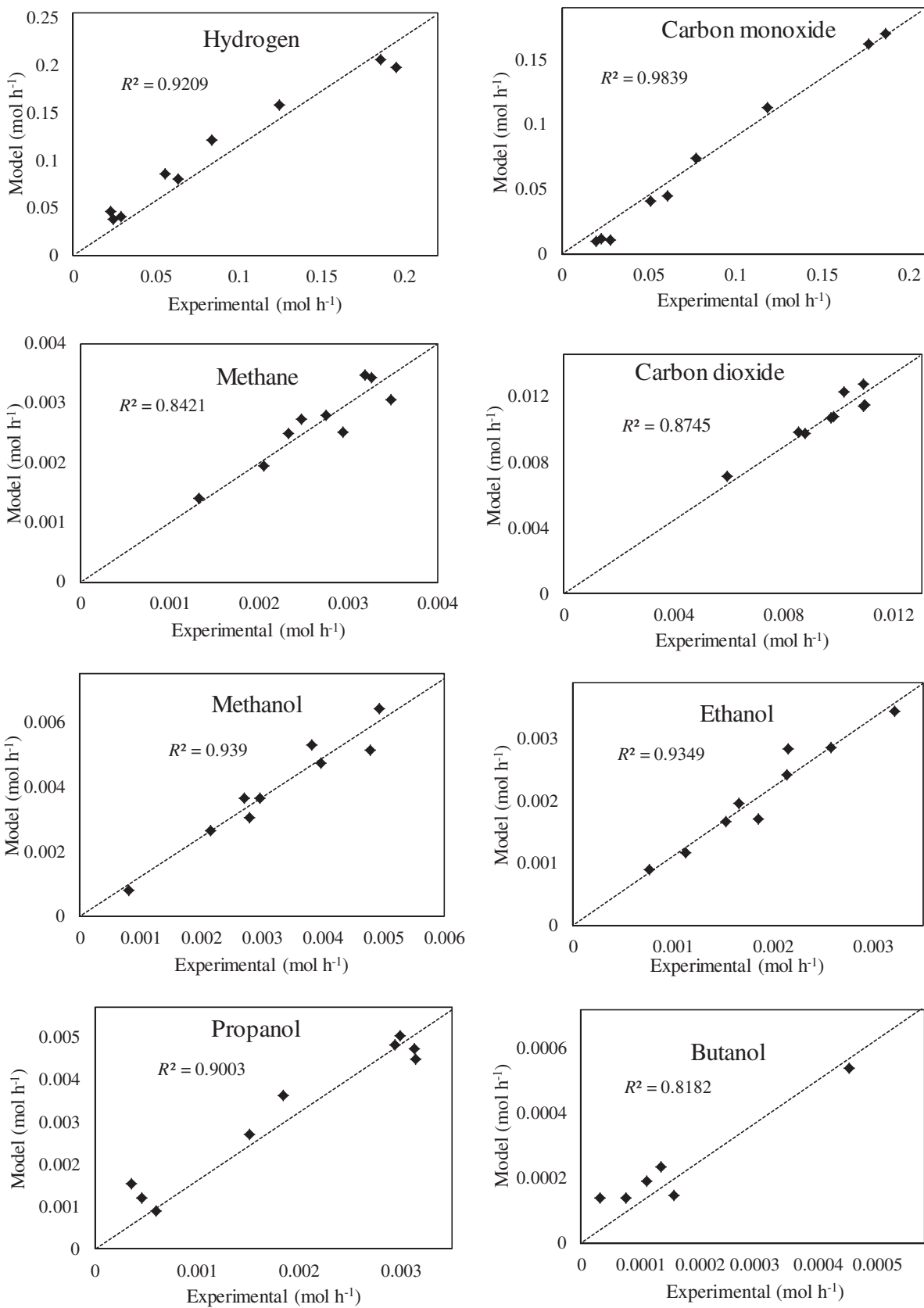


FIGURE 5 The overall reaction mechanism over alkali/MoS<sub>2</sub> catalysts<sup>14,29</sup>

TABLE 1 Kinetic parameters estimated based on model Equations (12)–(17)

Species	$A^a$	$E_a$ (kJ/mol)	Order of reaction species					$R^2$	Range of $E_a$ reported in literature (kJ/mol) <sup>b</sup>
			CO	H <sub>2</sub>	MeOH	EtOH	PrOH		
Methanol	0.0295	63	1.85	0.44	–	–	–	0.82	36-83
Ethanol	0.0102	54	0.75	1.39	0.24	–	–	0.83	38-83
Propanol	0.419	82	1.0	0.28	–	1.22	–	0.81	92-159
Butanol	5.201	104	0.63	0.08	–	–	0.59	0.88	107-148
Methane	5.812	126	–	0.6	0.83	–	–	0.81	112-118
Carbon dioxide	9.811	146	–	–	–	–	–	0.82	57-97

<sup>a</sup>Units (kmol/(kg s bars<sup>Σ</sup>reaction orders)).

<sup>b</sup>See Refs. 14, 19, 27, 28, 30, and 32.

## 4 | CONCLUSION

Kinetic modeling is an important tool to study the reaction kinetics, product distribution, and reactor performance. The application of kinetic models ranges between the simplest approach, such as power-law model and the highest degree of details, the microkinetic model. Models with less complexity are practical for reactor design, scale-up and process optimization. On the other hand, microkinetic models are complicated, but they are useful in case of design of new catalyst or improving the catalyst performance by providing insight into intermediates and preferred reaction pathways. However, in this study, our focus was on simplest approach providing information for reactor design and scale-up as the insight into the role and function of catalyst active sites was studied in our previous report.<sup>17</sup>

In this study, the formation of HAs over a cobalt-promoted MoS<sub>2</sub> catalyst was evaluated. The formation of both hydrocarbons and oxygenated products were observed over this catalyst system. The major oxygenated products were linear alcohols, such as methanol, ethanol, n-propanol, and n-butanol. The main hydrocarbon product was methane. Alcohol products (C<sub>3</sub>+) followed an ASF distribution and alcohol chain growth occur via a CO insertion mechanism. The results showed that liquid oxygenate formation can be maximized under optimum reaction condition: a temperature of 340°C, a pressure of 117 bar, GHSV of 27 000 mL g<sup>-1</sup> h<sup>-1</sup>, and H<sub>2</sub>/CO molar feed ratio of 1. A kinetic model based on the CO insertion mechanism was developed and we successfully estimated the reaction kinetics parameters within the range of reaction conditions in this study. An increase in activation energy with the length of alcohols was observed except for ethanol. Lower apparent activation energies of alcohols in comparison with hydrocarbon indicated that the catalyst is effective toward HAs formation. The lower activation energy agrees with the higher reaction rate of the reaction pathway, which means that reaction route is more efficient to take place over surface of solid catalyst. In other words,

catalyst active sites are more selective toward that reaction pathway with lower activation energy and higher reaction rate. The estimated activation energies and obtained optimum reaction conditions can be further employed to the design of an industrial reactor, optimizing the process operating conditions and improving the chemical plant economics.

## ACKNOWLEDGMENTS

Feng Zeng and Xiaoying Xi acknowledge China Scholarship Council (CSC) for financial support. Regina Palkovits and Leila Negahdar acknowledge the project house P2F (Competence Center Power to Fuel) of RWTH Aachen University financed by the Excellence Initiative of the German Federal and State Governments to promote science and research at German universities.

Open access funding enabled and organized by Projekt DEAL.

## ORCID

Leila Negahdar  <https://orcid.org/0000-0002-9119-6445>

Regina Palkovits  <https://orcid.org/0000-0002-4970-2957>

## REFERENCES

- Herman RG. Advances in catalytic synthesis and utilization of higher alcohols. *Catal Today*. 2000;55(3):233-245.
- Luk HT, Mondelli C, Ferré DC, Stewart JA, Pérez-Ramírez J. Status and prospects in higher alcohols synthesis from syngas. *Chem Soc Rev*. 2017;46(5):1358-1426.
- Angelici C, Weckhuysen BM, Bruijninx PCA. Chemocatalytic conversion of ethanol into butadiene and other bulk chemicals. *ChemSusChem*. 2013;6(9):1595-1614.
- Mascal M. Chemicals from biobutanol: technologies and markets. *Biofuels Bioprod Bioref*. 2012;6(4):483-493.
- Goldemberg J. Ethanol for a sustainable energy future. *Science*. 2007;315(5813):808-810.
- Green GJ, Yan TY. Water tolerance of gasoline-methanol blends. *Ind Eng Chem Res*. 1990;29(8):1630-1635.
- Iranmahboob J, Hill DO, Toghiani H. K<sub>2</sub>CO<sub>3</sub>/Co-MoS<sub>2</sub>/Clay catalyst for synthesis of alcohol: influence of potassium and cobalt. *Appl Catal A Gen*. 2002;231(1-2):99-108.

8. Li Z, Fu Y, Bao J, et al. Effect of cobalt promoter on Co-Mo-K/C catalysts used for mixed alcohol synthesis. *Appl Catal A Gen.* 2001;220(1-2):21-30.
9. Stevens R. Process for producing alcohols from synthesis gas. U.S. Patent, 4752622, 1988.
10. Stevens R, Conway M. Mixed alcohols production from syngas. U.S. Patent, 4831060, 1989.
11. Iranmahboob J, Hill DO. Alcohol synthesis from syngas over K<sub>2</sub>CO<sub>3</sub>/CoS/MoS<sub>2</sub> on activated carbon. *Catal Letters.* 2002;78(1-4):49-55.
12. Woo HC, Park TY, Kim YG, Nam IS, Lee JS, Chung JS. Alkali-promoted MoS<sub>2</sub> catalysts for alcohol synthesis: the effect of alkali promotion and preparation condition on. *Activ Select Surf Sci Catal.* 1993;75:2749-2752.
13. Woo HC, Park KY, Kim YG, Namau Jong, ShikChung IS, Lee JS. Mixed alcohol synthesis from carbon monoxide and dihydrogen over potassium-promoted molybdenum carbide catalysts. *Appl Catal.* 1991;75(1):267-280.
14. Santiesteban JG, Bogdan CE, Herman RG, Klier K, Mechanism of C<sub>1</sub>-C<sub>4</sub> alcohol synthesis over alkali/MoS<sub>2</sub> and alkali/Co/MoS<sub>2</sub> catalysts. In Proceedings of the 9th International Congress of Catalysis; 1988, pp. 561-568.
15. Klier K, Herman RG, Nunan JG, et al. Mechanism of methanol and higher oxygenate synthesis. *Stud Surf Sci Catal.* 1988:109-125.
16. Zeng F, Xi X, Cao H, Pei Y, Heeres HJ, Palkovits R. Synthesis of mixed alcohols with enhanced C<sub>3+</sub> alcohol production by CO hydrogenation over potassium promoted molybdenum sulfide. *Appl Catal B Environ.* 2019;246:232-241.
17. Xi X, Zeng F, Cao H, et al. Enhanced C<sub>3+</sub> alcohol synthesis from syngas using KCoMoS<sub>x</sub> catalysts: effect of the Co-Mo ratio on catalyst performance. *Appl Catal B Environ.* 2020;272:118950.
18. Patzlaff J, Liu Y, Graffmann C, Gaube J. Studies on product distributions of iron and cobalt catalyzed Fischer-Tropsch synthesis. *Appl Catal A Gen.* 1987;26(10):2122-2129.
19. Gunturu AK, Kugler EL, Cropley JB, Dadyburjor DB. A kinetic model for the synthesis of high-molecular-weight alcohols over a sulfided Co-K-Mo/C catalyst. *Ind Eng Chem Res.* 1998;37(6):2107-2115.
20. Weisz PB, Prater CD. Interpretation of measurements in experimental catalysis. *Adv Catal.* 1954;6(C):143-196.
21. Mears DE. Tests for transport limitations in experimental catalytic reactors. *Ind Eng Chem Process Des Dev.* 1971;10(4):541-547.
22. Fogler HS. *Elements of Chemical Reaction Engineering.* 5th ed. Upper Saddle River, NJ: Prentice Hall PTR; 2016.
23. Mears DE. Tests for transport limitations in experimental catalytic reactors. *Ind Eng Chem Process Des Dev.* 1971;10(4):541-547.
24. Calverley EM, Smith KJ. Kinetic model for alcohol synthesis over a promoted Cu/ZnO/Cr<sub>2</sub>O<sub>3</sub> catalyst. *Ind Eng Chem Res.* 1992;31(3):792-803.
25. Tronconi E, Ferlazzo N, Forzatti P, Pasquon I. Synthesis of alcohols from carbon oxides and hydrogen. 4. Lumped kinetics for the higher alcohol synthesis over a Zn-Cr-K oxide catalyst. *Ind Eng Chem Res.* 1987;26(10):2122-2129.
26. Nowicki L. Kinetics of CO hydrogenation on modified Cu/ZnO catalyst in a slurry reactor. *Chem Eng Process Process Intensif.* 2005;44(3):383-391.
27. Portillo MA, Perales ALV, Vidal-Barrero F, Campoy M. A kinetic model for the synthesis of ethanol from syngas and methanol over an alkali-co doped molybdenum sulfide catalyst: model building and validation at bench scale. *Fuel Process Technol.* 2016;151:19-30.
28. Su J, Mao W, Xu X-C, et al. Kinetic study of higher alcohol synthesis directly from syngas over CoCu/SiO<sub>2</sub> catalysts. *AIChE J.* 2014;60:1797-1809.
29. Smith KJ, Anderson RB. A chain growth scheme for the higher alcohols synthesis. *J Catal.* 1984;85(2):428-436.
30. Surisetty VR, Dalai AK, Kozinski J. Intrinsic reaction kinetics of higher alcohol synthesis from synthesis gas over a sulfided alkali-promoted Co-Rh-Mo trimetallic catalyst supported on multiwalled carbon nanotubes (MWCNTs). *Energy Fuels.* 2010;24(8):4130-4137.
31. Boahene PE, Dalai AK. Higher alcohols synthesis over carbon nanohorn-supported KCoRhMo catalyst: pelletization and kinetic modeling. *Ind Eng Chem Res.* 2018;57(16):5517-5528.
32. Christensen JM, Mortensen PM, Trane R, Jensen PA, Jensen AD. Effects of H<sub>2</sub>S and process conditions in the synthesis of mixed alcohols from syngas over alkali promoted cobalt-molybdenum sulfide. *Appl Catal A Gen.* 2009;366(1):29-43.
33. Newsome DS. The water-gas shift reaction. *Catal Rev.* 2006;21(2):275-318.
34. Park TY, Nam I-S, Kim YG. Kinetic analysis of mixed alcohol synthesis from syngas over K/MoS<sub>2</sub> catalyst. *Ind Eng Chem Res.* 1997;36(12):5246-5257.

## SUPPORTING INFORMATION

Additional supporting information may be found online in the Supporting Information section at the end of the article.

**How to cite this article:** Negahdar L, Xi X, Zeng F, Winkelman JGM, Heeres HJ, Palkovits R. CO hydrogenation over K-Co-MoS<sub>x</sub> catalyst to mixed alcohols: a kinetic analysis. *Int J Chem Kinet.* 2020;1-9. <https://doi.org/10.1002/kin.21453>